

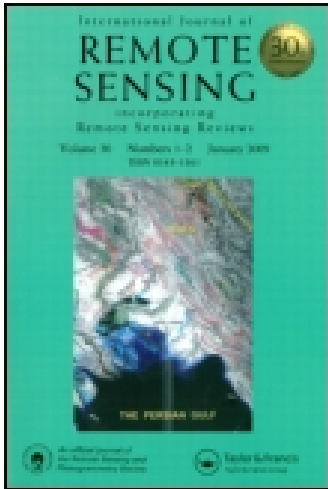
This article was downloaded by: [Columbia University]

On: 09 December 2014, At: 09:47

Publisher: Taylor & Francis

Informa Ltd Registered in England and Wales Registered Number:

1072954 Registered office: Mortimer House, 37-41 Mortimer Street,  
London W1T 3JH, UK



## International Journal of Remote Sensing

Publication details, including instructions for authors and subscription information:

<http://www.tandfonline.com/loi/tres20>

### Directional morphological image transforms for lineament extraction from remotely sensed images

N. K. Tripathi <sup>a</sup>, K. V. G. K. Gokhale <sup>a</sup> & M. U. Siddiqui <sup>b</sup>

<sup>a</sup> Department of Civil Engineering, I.I.T. Kanpur, Kanpur, 208 016, India

<sup>b</sup> Department of Electrical Engineering, I.I.T. Kanpur, Kanpur, 208 016, India

Published online: 25 Nov 2010.

To cite this article: N. K. Tripathi, K. V. G. K. Gokhale & M. U. Siddiqui (2000) Directional morphological image transforms for lineament extraction from remotely sensed images, International Journal of Remote Sensing, 21:17, 3281-3292, DOI: [10.1080/014311600750019895](https://doi.org/10.1080/014311600750019895)

To link to this article: <http://dx.doi.org/10.1080/014311600750019895>

PLEASE SCROLL DOWN FOR ARTICLE

Taylor & Francis makes every effort to ensure the accuracy of all the information (the "Content") contained in the publications on our platform. However, Taylor & Francis, our agents, and our licensors make no representations or warranties whatsoever as to the accuracy, completeness, or suitability for any purpose of the Content. Any opinions and views expressed in this publication are the opinions and views of the authors, and are not the views of or endorsed by Taylor & Francis. The accuracy of the Content should not be relied upon and should be independently verified with primary sources of information. Taylor and

Francis shall not be liable for any losses, actions, claims, proceedings, demands, costs, expenses, damages, and other liabilities whatsoever or howsoever caused arising directly or indirectly in connection with, in relation to or arising out of the use of the Content.

This article may be used for research, teaching, and private study purposes. Any substantial or systematic reproduction, redistribution, reselling, loan, sub-licensing, systematic supply, or distribution in any form to anyone is expressly forbidden. Terms & Conditions of access and use can be found at <http://www.tandfonline.com/page/terms-and-conditions>

## Directional morphological image transforms for lineament extraction from remotely sensed images

N. K. TRIPATHI, K. V. G. K. GOKHALE

Department of Civil Engineering, I.I.T. Kanpur, Kanpur-208 016, India;  
e-mail: nitin@iitk.ernet.in

and M. U. SIDDIQUI

Department of Electrical Engineering, I.I.T. Kanpur, Kanpur-208 016, India

**Abstract.** Morphological image transforms find their basis in the notions of mathematical morphology. An attempt is made to develop morphological transforms for enhancement of directional edges and lineaments from satellite imagery. Geostructural features are generally oriented in preferred directions. This information has been utilized in designing structuring elements for morphological transforms. Several shapes and sizes of structuring elements have been designed and applied to delineate lineaments in different litho-environments of the same study area. Top hat transform has been applied using the directional structuring elements for edge image at  $0^\circ$ ,  $30^\circ$ ,  $60^\circ$ ,  $90^\circ$ ,  $120^\circ$  and  $150^\circ$ . Geological lineaments such as faults could be easily identified on an edge image obtained using top hat transformation followed by an image superimposition technique. The lineament map was developed using directionally enhanced edge images and the results have been verified.

### 1. Introduction

The general trend in digital image processing in remote sensing has been to adopt conventional edge operators or enhancement techniques. Qari (1991) used classical image processing such as principal component analysis, decorrelation stretching and highpass filtering for lineament enhancement adopting Landsat TM data. The study revealed the directional nature of geologic lineaments and emphasized the need for directional filtering. Mah *et al.* (1995) also adopted an algorithm for enhancing the lineaments in particular directions to obtain maximum mapping efficiency. However, minor lineaments oriented in directions other than that of the main fault could not be enhanced. The complex mathematical and statistical nature of conventional filters distort the basic shape and size of inherent features in remotely sensed images. Although directional edge operators are available, their adaptability in the case of natural surface features has not been established. Image processing based on mathematical morphology is explored in this paper for enhancement of directional lineaments. In this case an image is understood to be a set of natural or real numbers which is constituted by a number of subsets comprising numerous structuring elements. These

---

Paper presented at ICORG '97 International Conference on Remote Sensing and GIS/GPS, Hyderabad, India, 18–21 June 1997.

subsets have a relationship which can be described using the notions of set theory (Matheron 1975, Serra 1982, 1986, Giardina and Dougherty 1988). Morphological image processing has been utilized in many areas and has gained prominence in recent years. Conrad (1972) employed principles of mathematical morphology for studying the permeability characteristics of petroleum rocks using the simulation of a set of geological faults (Serra 1982). Photographs of dust particles have been used to understand their size distribution and shape characteristics (Klein and Serra 1973).

In the recent past, scientists in the area of remote sensing have initiated studies involving morphological image processing for feature identification in satellite imagery (Ansoult *et al.* 1990, Vincent and Soille 1991). Morphological transforms have been generally applied for the binary image case (Ghosh 1988, Haralick *et al.* 1989, Maragos and Ziff 1990). Remotely sensed digital images are multilevel, i.e. in greyscale. Sternberg (1986) presented a generalization of the morphological operations of *erosion*, *dilation*, *opening* and *closing* for the greyscale image case. The same concept is being adopted and explored here for remotely sensed greyscale images obtained from the Indian Remote Sensing Satellite (IRS-1B). In the present work the possibility of employing the concept of morphological image processing for remotely sensed satellite data for enhancing structural features is primarily explored.

## 2. Study area and data used

The north-eastern part of the Singrauli coal basin, lying in central India, was chosen as the study area. This area is marked with several faults and a dense network of geological lineaments. The sequence within the coalfield in this region is essentially of Lower Gondwana Formations. A major fault traversing in an east–west direction is located in the northern part of the basin. This limits the northern boundaries of coal seams and also marks the boundary of metamorphic and Barakar sandstone zones. Govind Ballabh reservoir is situated in the south-east of the study area. There are nine coal-mining blocks: Jhingurdah, Kakri, Bina, Marrak, Dudhichua, Jayant, Nigahi, Khadiya and Amolori. Open-cast mining is adopted in this area because coal is available at shallow depth. The general location and geological settings are shown in figure 1.

It has been suggested by earlier workers that the red band (0.6–0.7  $\mu\text{m}$ ) offers better differentiation of soil and geological boundaries (Jensen 1986). Data from the Indian Remote Sensing Satellite (IRS -1B) of path 23 and row 51 of Band 3 (0.62–0.68  $\mu\text{m}$ ) has been used in the present work. A Band 3 image of the study area is shown in figure 2. The Bijul river is seen in the upper left corner. This river is structurally controlled by the Vindhyan ridges. The major boundary fault can be seen distinctly traversing across the centre of the image from east to west. The coal-mining blocks are arranged in garland fashion and situated to the south of this fault. As detailed in figure 1, the tone and texture variation for metamorphic and Barakar zones is observed in figure 2. This area is full of major and minor lineaments in addition to other geomorphic and geostructural details.

The toposheet at 1:250 000 from the Survey of India and the geological map at the same scale from the Geological Survey of India were used. In addition, several maps generated by Coal India Limited after field mapping were also utilized for the present study.

## 3. Morphological transformations

Satellite imagery is used for obtaining information on inherent objects and efforts have been directed towards maximizing information retrieval. Human vision fails to

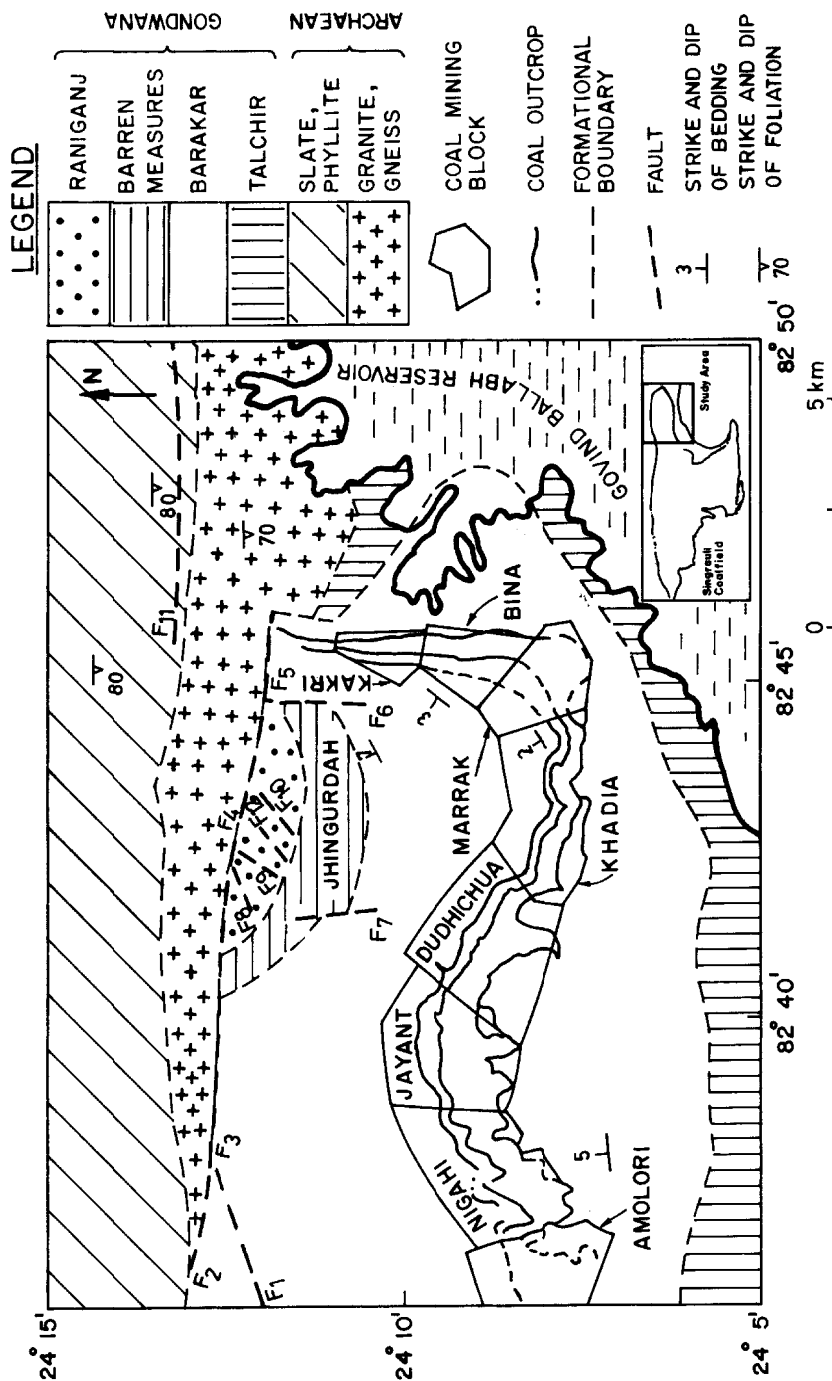


Figure 1. North-eastern part of the Singrauli coal basin (modified from SOI and GSI maps).

accomplish this task efficiently due to its spectral and spatial constraints (Gonzalez and Wintz 1977). Digital image processing can alleviate this limitation to a larger extent by enhancing the quality of the image. *Morphological transformations* attempt to establish a spatial relationship between image subsets. These are referred to as image *objects*. In morphological image processing the basic set selected to identify any larger image subset of the principal image  $Z$  is very important. This basic set is termed as a *structuring element*.

In an image space  $Z$  for each of its points  $i$ , a separate structuring element  $h(i)$  can be associated. An image can be modified to various forms by changing the *structuring element* or the *transformation types*.

The principles of mathematical morphology have also been extended to the greyscale image case. Greyscale images are described as a grey level function  $f(x, y)$  on the points of Euclidean 2-space. In Euclidean 3-space the grey level function is considered as a set of points  $[x, y, f(x, y)]$  imagined as a thin, undulating and not necessarily a continuous sheet. A greyscale image is described in terms of mathematical morphology by an umbra  $U(f)$  in Euclidean 3-space, where a point  $p$  with its coordinates  $(x, y, z)$  belongs to the umbra if and only if  $z \leq f(x, y)$ . In image processing the umbrae are very significant as they remain umbrae even after morphological operations such as union, intersection, dilation or erosion are performed. Sternberg (1986) extended the fundamental morphological operations of dilation, erosion, opening and closing from the binary image case to the greyscale images as explained in following subsections.

### 3.1. Dilation

The dilation of a set  $X$  by structuring element  $Y$  can be expressed as:

$$X \oplus Y = \bigcup_{y \in Y} X_y \quad (1)$$

The dilation of  $U[a]$  by  $B$  is the union of translations of  $U[a]$  by points of  $B$ . At a given location  $(x, y)$  the grey levels  $d(x, y)$  of the dilation are determined by the maxima of the translated umbra  $U[a]$ . Although  $U[a]$  is translated by all the points

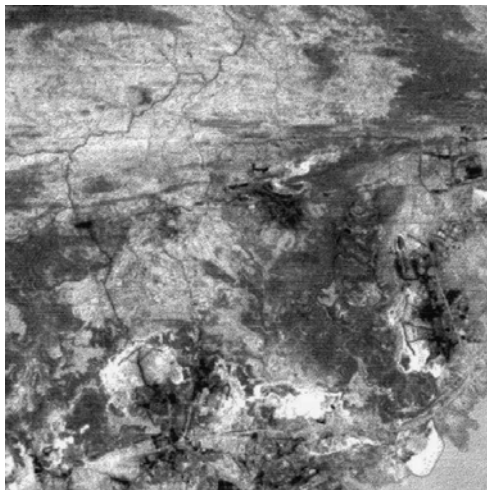


Figure 2. IRS 1B LISS II Band 3 image of the Singrauli coalfield.

of  $B$ , only those points lying on the surface of  $B$  can create maxima. The dilated greyscale image is computed then, as the maximum of the sum of grey levels of  $b(x, y)$ , the function describing the surface of  $B$ , with each of the points of  $a(x, y)$ .

$$d(x, y) = \max_{i, j} [a(x - i, y - j) + b(i, j)] \quad (2)$$

### 3.2. Erosion

The erosion of a set  $X$  by structuring element  $Y$  can be expressed as

$$X \ominus Y = \bigcap_{y \in Y} X_y \quad (3)$$

The erosion of  $U[a]$  by  $B$  is likewise determined as a difference of the grey levels of  $b(x, y)$  and points of  $a(x, y)$ , the grey levels of the eroded image  $e(x, y)$  determined by the minimum over all the points of  $b(x, y)$ .

$$e(x, y) = \min_{i, j} [a(x - i, y - j) - b(-i, -j)] \quad (4)$$

The expressions for greyscale dilation and erosion bear a marked similarity to the convolution integral encountered frequently in digital image processing, with sums and differences replacing multiplication and minimum and maximum replacing summation. Image processing through iterative morphological transformation is a process of selective information removal where irrelevant image content is irrecoverably destroyed, enhancing the contrast of the essential image features.

### 3.3. Opening

The opening of  $X$  by  $Y$  is defined in terms of an erosion followed by a dilation. Mathematically it can be represented as:

$$X_Y = [X \ominus Y] \oplus Y \quad (5)$$

The opening of  $X$  by  $Y$  is the union of translation of  $Y$  completely contained in  $X$ .

### 3.4. Closing

The closing of  $X$  by  $Y$  is a dilation followed by an erosion. Mathematically it can be represented as:

$$X^Y = [X \oplus Y] \ominus Y \quad (6)$$

The closing of  $X$  by  $Y$  is the complement of the translations of  $Y$  completely contained in  $X^c$ .

Greyscale images opened and closed by three-dimensional structuring elements are transformed in predictable and useful ways. Rotationally symmetric structuring elements are often employed for opening transformations because the results do not depend on the orientation of the image. These transforms utilize sequences of operations involving dilation, erosion and difference for detecting edges and are non-reversible in nature.

## 4. Morphological edge detection

Most of the transforms available for edge detection are based on the basic operations of dilation and erosion. Techniques adopted for edge detection in satellite imagery are discussed as follows.

4.1. Edge detection based on dilation

The digital satellite image  $f(x, y)$  is dilated using structuring element  $h(i, j)$ . The original image (figure 2) is subtracted from this *dilated* image. The resultant transformed image  $g(x, y)$  reveals a large number of edges. It is noticed by visual inspection that outer boundaries of the objects are emphasized. Mathematically the process is as follows:

$$\text{DILATE}[f(x, y)] = f(x, y) \oplus h(i, j) \tag{7}$$

$$g(x, y) = \text{DILATE}[f(x, y)] - f(x, y) \tag{8}$$

Therefore, this process seems to be relevant for extracting the geological boundaries of various formations and other geomorphic units marked by outer peripheral boundaries.

4.2. Edge detection based on erosion

In another approach image  $f(x, y)$  is *eroded* using structuring element  $h(i, j)$ . The eroded image is subtracted from the original image and the transformed image  $g'$  revealed a large number of edges.

$$\text{ERODE}[f(x, y)] = f(x, y) \ominus h(i, j) \tag{9}$$

$$g'(x, y) = f(x, y) - \text{ERODE}[f(x, y)] \tag{10}$$

The edge output using this method brings out mainly inner boundaries and numerous noisy edge contours. The abundance of inner edges of surface features hinders visual interpretation of lineaments and geostructural features like faults. Several structuring elements of size  $3 \times 3$  and  $5 \times 5$  having solid, ring, plus and diagonal shapes at  $45^\circ$  and  $135^\circ$  (figure 3) have been applied and it is found that in the case of the present image, the  $3 \times 3$  plus shape structuring element offers edge image with less noise and more interpretability.

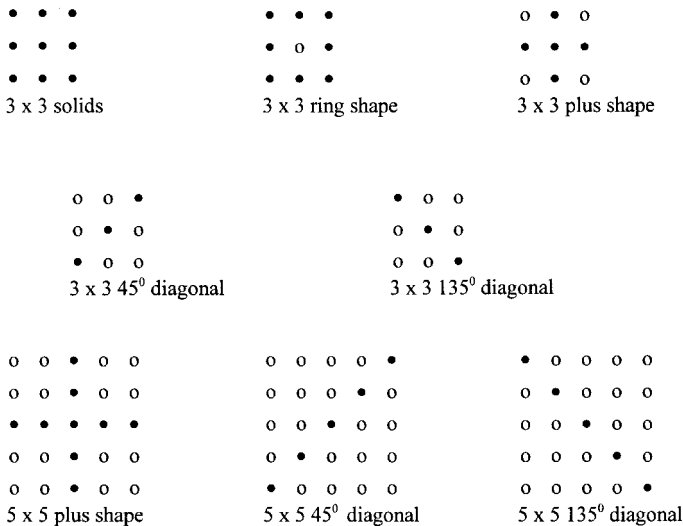


Figure 3. Structuring elements used in edge detection.

#### 4.3. Edge detection using top hat transformation

Edge detection is achieved using transformations involving operations of *closing* and *difference*. This technique is known as *top hat transformation*. Top hat morphological transformation extracts *topographical peaks* or *valleys* from a digital image. An explanation of the process is illustrated in figure 4. Top hat transformations are developed for the binary image case. In the present study an attempt is made to apply it to the case of the greyscale remotely sensed image.

The top hat transformation based on the *close* operation is expressed mathematically as follows:

$$\text{Top hat } (f) = f^B - f \quad (11)$$

where  $f^B$  is an image obtained after performing the *close* operation on image  $f$ .

The top hat transformation based on the *open* operation is expressed mathematically as follows:

$$\text{Top hat } (f) = f - f_B \quad (12)$$

Where  $f_B$  is an image obtained after performing the *open* operation on image  $f$ .

For extraction of structural features such as faults, folds, fractures and lineaments, a transformation involving closing and difference with the original image is expected to yield better results than the one involving opening and difference operations. In geologic imagery, near the structural features such as faults, fractures are marked by a moist zone containing soil, a granular zone and vegetation, characterized by a sudden drop in grey level values due to much lower reflectance than rock features. Therefore, the main object while targeting edges is to filter out topographic valleys. As illustrated in figure 4, the topographic valleys are filtered using the top hat transformation based on the *close* operation.

The top hat transformation should be applied in all possible directions as the orientation of linear features in a new geological image is unknown. The structuring element  $h(i, j)$  influences the final output due to its size and shape. Several such elements can be designed to obtain an output closer to the desired one. This transformation is performed using a sequence of closing by three structuring elements

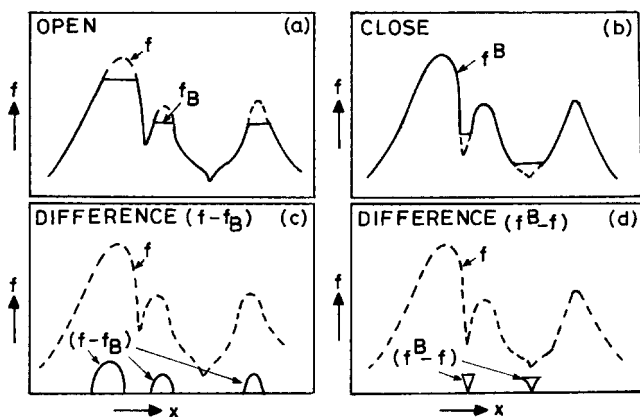


Figure 4. Top hat transformation using closing and difference operations.

with directions 0°, 60°, 120° and also the complementary structuring elements in the directions 30°, 90°, 150° followed by the differencing operation with the original image. The structuring elements used have hexagonal shape as shown in figure 5. In these, *structuring elements*, the main active cellular elements are positioned at the desired orientation.

These edge transforms are applied on IRS-1B LISS II image as shown in figure 2. The result of transformation using a structuring element at 0° direction on the input image appeared very noisy. The other directions in which the transformation was applied were 60°, 120°, 30°, 90° and 150° which displayed distinct edges. The edge image obtained using top hat 60° and 120° are shown in figures 6 and 7.

4.4. *Edge detection using top hat transformation and image superimposition*

It was found that top hat transformation could bring out edges very prominently in various directions. These edge outputs may be used for interpreting lineaments. Lineaments such as faults, fractures, dissected zones and joints are delineated on the satellite imagery using certain visual keys like isolated linear vegetation trend, drainage pattern and moisture in comparatively dry regions (Lillesand and Kiefer 1979). These cover types resulting from the presence of moisture are associated with low grey levels. In the present work the original image comprising all natural

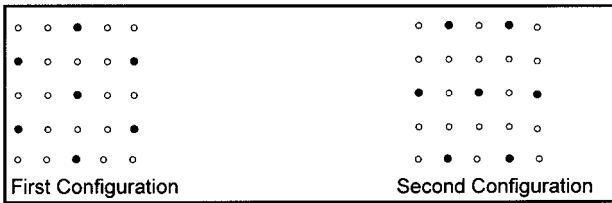


Figure 5. Hexagonal structuring elements for directional edge detection in top hat transformation.



Figure 6. Edge image using top hat transformation at 60°.

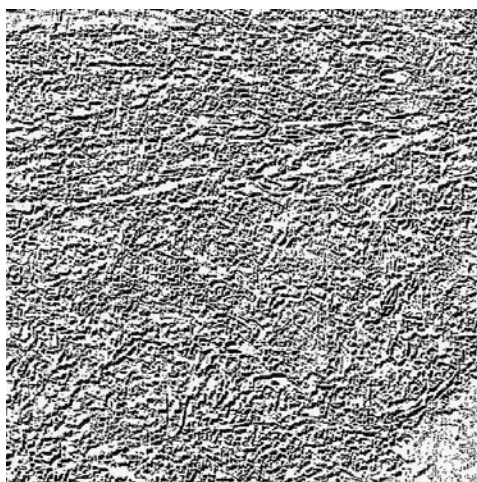


Figure 7. Edge image using top hat transformation at 120°.

features was superimposed on the edge output of the top hat transformation. The methodology adopted here was as follows:

Step 1. CLOSE operation on the image  $f$ ;

Step 2. Subtract the original image from the output image of step 1;

Step 3. Compare each pixel of top hat ( $f$ ) and original image ( $f$ ) and replace the pixel of the top hat image if there exists a minima in the original image.

$$\text{EDGE}(f) = \text{MIN} [\{\text{Top hat}(f)\}, f] \quad (13)$$

This method was attempted involving several structuring elements and the best results were obtained in the case of 45°, 135° and plus shape structuring elements of size three (figure 3). In the case of other structuring elements of larger size, fewer edges were obtained and other configurations of structuring elements rendered noisy edge image, which is unsuitable for lineament mapping. The edge image with best visual appearance emphasizing the edges and lineaments was rendered by the 3 × 3 plus shape structuring element (figure 8).

## 5. Results and discussions

Four transformations for edge detection were employed in the present study. The *first approach* involving image *differencing* and *dilation* helped in extracting exterior boundaries, whereas the *second approach* of difference of the original image and eroded image yielded interior edges. The first transformation involving dilation is more useful in the case of geologic images for delineation of formation boundaries and detecting main boundary faults. Several structuring elements were used but the acceptable results were found with the plus shape element 3 × 3. The edge image produced by the second approach appeared difficult to interpret as a large number of inner edges were produced.

The *third approach* for edge detection was *top hat transformation*. Hexagonal structuring elements of size six were employed to enhance the edges in various directions like 0°, 60°, 120°, 30°, 90° and 150°. The edge output showing grey and white shades offers distinct impressions of edges (figures 6 and 7). The discontinuities



Figure 8. Edge image using top hat transformation and image superimposition using the plus shape  $3 \times 3$  structuring element.

and lineaments are better perceived in these edge images. A combined analysis of edge images in various directions as mentioned above offer better visual delineation of lineaments.

The *fourth approach* of edge detection proposed included image *superimposition* as a modification over *top hat transformation*. Three structuring elements ( $45^\circ$ ,  $135^\circ$  and plus shape  $3 \times 3$ ) were utilized which yielded encouraging response by emphasizing the moist zones near the geostructural lineaments. If the size of structuring element is increased, a blurring effect is caused in the edge output. Edge output from the plus shape  $3 \times 3$  transform is shown in figure 8. The output obtained using this process offered the most encouraging edge image on which faults and lineaments could be easily identified. This method provides an efficient tool to distinguish between physical objects (roads, railway lines, built-up and other man-made linear features) and geo-structural features. A geostructural map (figure 9) has been prepared based on edge images from top hat  $30^\circ$ ,  $60^\circ$ ,  $90^\circ$ ,  $120^\circ$ , and  $150^\circ$  and image superimposition techniques at  $45^\circ$ ,  $135^\circ$ , and plus shape structuring elements. In this map, major boundary faults along with other orthogonal faults are illustrated. In Jingurdah, Kakri, Bina, Marrak and Khadia, a large number of faults are located. Mines in this area are situated in a garland shape and the structural features tend to limit their extent. Maps from Coal India Limited and the Geological Society of India contain these faults. Formation boundaries of metamorphics, Barakar and Talchir have also been mapped from distinct tonal and textural variations. The periphery of Sardar Ballabh reservoir is also mapped in the bottom right corner of the image.

## 6. Conclusions

Morphological transformation involving top hat transformation employing a hexagonal structuring element for multi-direction  $0^\circ$ ,  $60^\circ$ ,  $90^\circ$ ,  $120^\circ$  and  $150^\circ$  can be used for enhancement of directional lineaments. In this process, man-made linear features like roads and canals could be avoided by using top hat transformation and image superimposition techniques. Geostructural details (figure 9) mapped using this

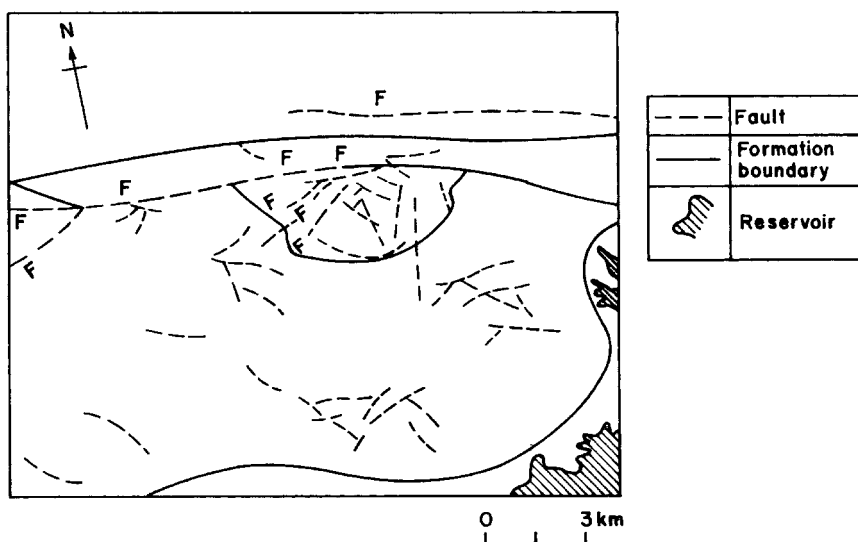


Figure 9. Geostructural map produced based on morphological transformation.

approach have been verified from the published maps of the Geological Society of India (GSI) and Coal India Limited (CIL). Most of the major faults mapped in figure 9 are confirmed by GSI and CIL maps. In addition, several new faults were also interpreted. The results of *visual delineation* of lineaments presented in figure 9 are exploratory in nature. Although, major lineaments have been confirmed, the reliability of minor faults and lineaments is yet to be established by appropriate detailed field exploration.

The present approach of mathematical morphology has yielded satisfactory results. It seems to be better suited for digital enhancement of lineament based on its unique characteristics of preserving the basic morphology and homotopy of the image by a proper choice of structuring elements and not involving complex mathematical and statistical operations as adopted in conventional image processing techniques. The success obtained in enhancing the linear features in the present study indicates the potential for future development of *structuring elements* and *transformations* for extraction and delineation of geomorphic features in addition to geostructural features from satellite imagery.

### Acknowledgments

The authors extend their sincere gratitude to engineers and staff of Coal India Limited for their help in conducting the field verification and collecting the ground data. The authors are grateful to the Department of Civil Engineering, Indian Institute of Technology Kanpur, India and Ministry of Human Resource Development, India for funding this work at different stages and providing the necessary infrastructure. We are obliged to the Coal Mining Planning and Design Institute (CMPDI), India, for help provided during field verification of lineaments in the Singrauli coal basin.

## References

- ANSOULT, M. M., SOILLE, P. J., and LOODTS, J. A., 1990, Mathematical morphology: A tool for automated GIS data acquisition from scanned thematic maps. *Photogrammetric Engineering and Remote Sensing*, **56**, 1263–1271.
- GHOSH, P. K., 1988, A mathematical model for shape description using Minkowski operators. *Computer Vision Graphics and Image Processing*, **44**, 239–269.
- GIARDINA, C. R., and DOUGHERTY, E. R., 1988, *Morphological Methods in Image and Signal Processing* (New Jersey: Prentice Hall).
- GONZALEZ, R. C., and WINTZ, P., 1977, *Digital Image Processing* (Massachusetts: Addison Wesley).
- HARALICK, R. M., XINHUA, Z., LIN, C., and LEE, J. S. J., 1989, The digital morphological sampling theorem. *IEEE Transactions on Acoustics, Speech and Signal Processing*, **37**, 2067–2089.
- JENSEN, J. R., 1986, *Introductory Digital Image Processing* (New Jersey: Prentice Hall).
- KLEIN, J. C., and SERRA, J., 1973, The texture analyser. *Journal of Micro-optics*, **95**, 349–356.
- LILLESAND, T. M., and KIEFER, R. W., 1979, *Remote Sensing and Interpretation* (New York: John Wiley).
- MAH, A., TAYLOR, G. R., LENNOX, P., and BALIA, L., 1995, Lineament analysis of Landsat TM images, Northern Territory, Australia. *Photogrammetric Engineering and Remote Sensing*, **61**, 761–773.
- MARAGOS, P., and ZIFF, R. D., 1990, Threshold superposition in morphological image analysis systems. *IEEE Transactions on Pattern Analysis and Machine Intelligence*, **12**, 498–504.
- MATHERON, G., 1975, *Random Sets and Integral Geometry* (New York: John Wiley).
- QARI, M. Y. H. T., 1991, Application of Landsat TM data to Geological Studies, Al-Khabt area, Southern Arabian Shield. *Photogrammetric Engineering and Remote Sensing*, **57**, 421–429.
- SERRA, J., 1982, *Image Analysis and Mathematical Morphology* (London: Academic Press).
- SERRA, J., 1986, Introduction to mathematical morphology. *Computer Vision Graphics and Image Processing*, **35**, 283–305.
- STERNBERG, S. R., 1986, Grayscale morphology. *Computer Vision Graphics and Image Processing*, **35**, 333–355.
- VINCENT, L., and SOILLE, P., 1991, Watersheds in digital spaces: an efficient algorithm based on immersion simulation. *IEEE Transactions on Pattern Analysis and Machine Intelligence*, **13**, 583–598.